PHYSICAL REVIEW E VOLUME 48, NUMBER 6 DECEMBER 1993

Visualizing the collective motions responsible for the α and β relaxations in a model glass

Peter Harrowell
*Van 't Hoff Laboratory for Physical and Colloid Chemistry, University of Utrecht, Padualaan 8, 3584 CH Utrecht, The Netherlands and Department of Physical and Theoretical Chemistry, University of Sydney, Sydney, New South Wales 2006, Australia**

(Received 6 July 1993)

Maps of the spatial distributions of the relaxation times are obtained from Monte Carlo simulations of the facilitated kinetic Ising model. The β relaxation, acting over short and intermediate time scales, is observed to occur in localized pockets. The slow α relaxation is governed by the fraction of these pockets which are free to move. This physical picture is able to account for the non-Arrhenius temperature dependence of the time scales of the α process, the scaling of the relaxation function in the β region, and the value of the relaxation function at the crossover time.

PACS number(s): 61.20.Ja, 64.70.Pf

I. INTRODUCTION

In this paper we examine the spatial correlations of the relaxation-time distribution obtained from computer simulations of a model glass. The model, a version of the kinetic Ising model described below, is shown to exhibit a number of the characteristic features of relaxation of a "fragile" liquid [1]. These include a non-Arrhenius temperature dependence of the relaxation time and a two-step decay of the spin correlations with time. If a glass is defined in terms of its phenomenology, then this model, simple as it is, is a glass and the description of the relationship between spatial fluctuations and the form of the relaxation function is of general interest. Much of the recent experimental [2] and simulation [3] studies of relaxation in glasses has been designed around the predictions of the recently developed mode-coupling theory [4]. We present this work as a complementary approach, based on a treatment of the complex dynamics in real space rather than the Fourier space used in Ref. [4]. The major results reported here are (i) an explicit determination of the spatial features of the relaxation-time distribution in a glassy system, and (ii) the demonstration that this physical picture permits a unified quantitative analysis of the intermediate-(β) and long-time (α) domains of the relaxation function. While there are yet no direct experimental measurements of such spatial fluctuations of the relaxation rates, a recent "reduced" four-dimensional (4D) exchange NMR experiment [5] on poly(vinyl acetate) has indicted that some sort of heterogeneity exists for time scales at least up to the average relaxation time.

II. THE MODEL AND ITS PHENOMENOLOGY

The model used in this work, a version of the kinetic Ising model, has been described elsewhere [6,7]. Briefly, the facilitated kinetic Ising (fkI) model consists of a quantity, the "spin," distributed discretely over the vertices of a two-dimensional (2D) square lattice. At each site the spin can take one of two values, $\sigma_i=-1$ (down) or 1 (up). The spins do not interact so that, in the presence of a field h, the energy is simply

$$E=\sum_{k=1}^{N}\sigma_i h\ . \tag{1}$$

The cooperativity in this model is of a kinetic nature and is introduced in the master equation which governs the stochastic dynamics. The transition probabilities for spin flips depend strongly on the state of the neighboring spins. Specifically, the probability that spin i will flip from σ_i to $-\sigma_i$ is given by

$$W_i(\sigma_1,\dots,\sigma_i,\dots,\sigma_N)\propto m_i(m_i-1)\exp[h(\sigma_i-1)/k_BT]\ , \tag{2}$$

where m_i is the number of the four nearest-neighbor spins which are up. The consequence of Eq. (2) is that a spin cannot flip unless two or more of its neighbors are up, resulting in kinetics which are strongly constrained by the local configurational fluctuations. The transition to a glass arises as the reduced temperature T^* $(=k_BT/h)$ is lowered so that the equilibrium concentration of up spins, $c=1/[1+\exp(2/T^*)]$, decreases, leading to a rapid slowing down of relaxation. The fkI model was simulated using a Monte Carlo algorithm described previously [6,7]. Relaxation functions were obtained as the average of 30 runs on a 50×50 lattice with periodic boundary conditions. A unit of time corresponds to 2500 spin-flip attempts. The relaxation function used here, $F(t)$, is defined as the fraction of spins which remain unflipped after a time t and is related to the distribution of first flip times $P(t)$ by the relation $P(t)=-dF(t)/dt$.

The facilitated kinetic Ising model represents one of the simplest models in which relaxation kinetics are governed by strong local kinetic constraints. If there is some form of general universality in the origin of glassy dynamics, then it is possible that such a simple model may be sufficient to capture the important physics. Questions of universality aside, the fkI model exhibits a number of the important phenomena characteristic of glassy

---

*Permanent address.

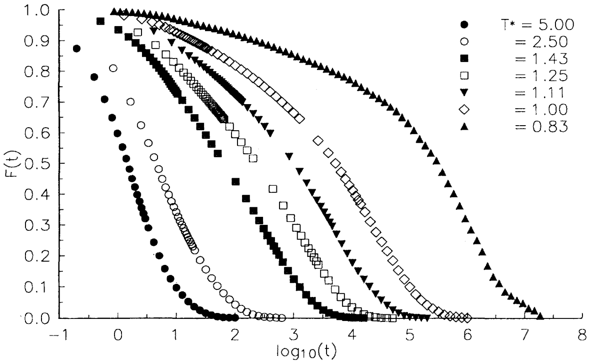

FIG. 1. The relaxation function $F(t)$ plotted against $\log_{10}(t)$ for $1/T^*=0.2$, 0.4, 0.7, 0.8, 0.9, 1.0, and 1.2 (corresponding to $T^*=5.00$, 2.50, 1.43, 1.25, 1.11, 1.00, and 0.83, respectively).

relaxation (these are described below). Understanding how such behavior can arise in even a simple model as a result of microscopic fluctuations and local constraints without the intrusion of uncontrolled assumptions remains an important problem.

The relaxation functions $F(t)$ are presented in Fig. 1 for reduced temperatures T^* between 0.83 and 5.00. The stretching of the time scale with decreasing temperature, evident in the relaxation functions, is quantified in terms of a relaxation time τ_L [defined as the area under $F(t)$], which is shown in Fig. 2. As can be seen, τ_L exhibits a strong non-Arrhenius temperature dependence similar to many glass formers characterized by relatively weak molecular interactions. Replotting the relaxation function $F(t)$ against a time scaled by the relaxation time τ_L in Fig. 3 reveals that at long times the relaxation function has a temperature-independent form. Similar observations have been made previously of real [8] and simulated [3] glasses and are considered characteristic of the α relaxation. An empirical functional form, $A\exp[-(t/\tau_L)^\gamma]$, which has been found to fit a wide variety of relaxation data [8], provides a reasonable fit to $F(t)$ at long times (see Fig. 3). Independent of any choice of fitting function, the breakdown of the scaling relation at short times indicates that some sort of crossover occurs to a different physical process in the intermediate-time region. In the discussion that follows, t^* will be used to denote the crossover time.

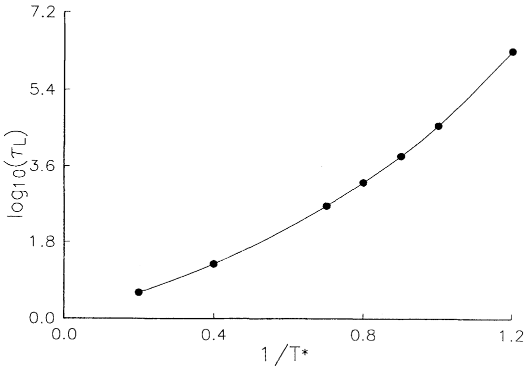

FIG. 2. $\log_{10}(\tau_L)$ is presented as a function of $1/T^*$, clearly exhibiting a non-Arrhenius temperature dependence.

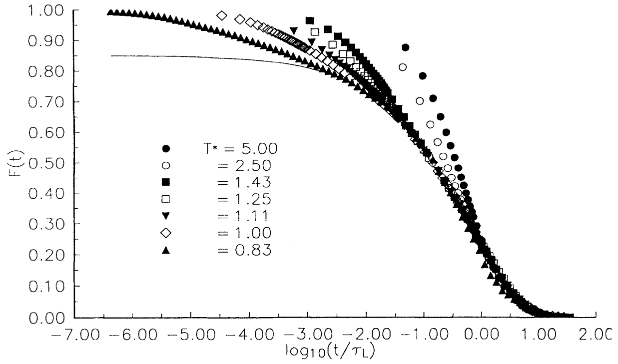

FIG. 3. The relaxation function $F(t)$ vs $\log_{10}(t/\tau_L)$ for the same temperature as shown in Fig. 1. Note the appearance of a common curve at long times. The solid line is a fitted stretched exponential function, $0.85\exp[-(t/\tau_L)^{0.48}]$.

III. VISUALIZING THE COLLECTIVE RELAXATION

We can explore the processes giving rise to relaxation at any time scale by looking at the maps of the spatial distribution of the first flip time τ of each spin for a given run. Maps depicting the distribution of τ over the 50×50 lattice are presented in Figs. 4 and 5 for a low ($T^*=0.83$) and a high ($T^*=1.67$) temperature, respectively. Shading is used to indicate the magnitude of the first flip time at a given lattice point, with white and light gray denoting regions with $\tau<t^*$ and dark gray and black indicating a $\tau>t^*$. These maps provide an extraordinarily detailed picture of the relaxation processes in glasses. A study of their scaling properties has been presented elsewhere [9]. At a low temperature (Fig. 4),

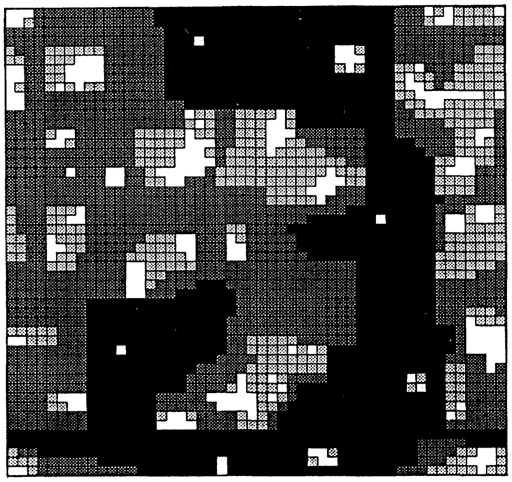

FIG. 4. A map of the distribution of first flip times τ among the sites on a 50×50 lattice at a low temperature, $T^*=0.83$. The magnitude of τ is represented as follows: $\log_{10}(\tau)<2.0$ (white), $2.0<\log_{10}(\tau)<3.76$ $[=\log_{10}(t^*)]$ (light gray), $3.76<\log_{10}(\tau)<6$ (dark gray) and $6<\log_{10}(\tau)$ (black). Note the isolated rectangles of fast spins indicating trapped pockets.

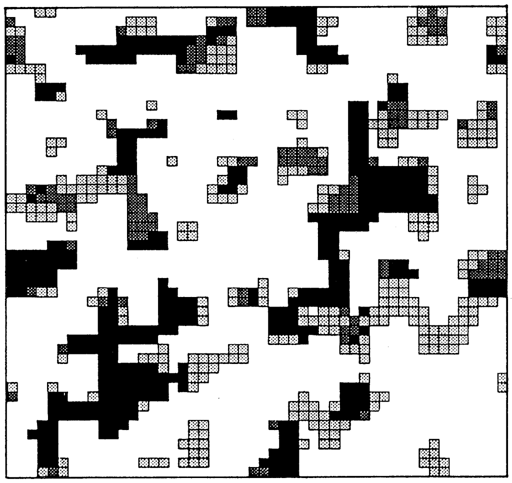

FIG. 5. A map of the distribution of first flip times τ among the sites on a 50×50 lattice at a high temperature, $T^*=1.67$. The magnitude of τ is represented as follows: $\log_{10}(\tau)<0.8$ (white), $0.8<\log_{10}(\tau)<1.85$ $[=\log_{10}(t^*)]$ (light gray), $1.85<\log_{10}(\tau)<2.8$ (dark gray), and $2.8<\log_{10}(\tau)$ (black).

relaxation begins in localized pockets scattered through the sample (white regions). At later times (shaded light gray) up to the crossover time t^*, the relaxation around a fraction of these pockets has run up against surrounding "walls" of down spins which prevent further relaxation by that site. These trapped pockets can be seen on the map as isolated rectangular regions of short relaxation times bounded by regions of substantially longer time scales. A small fraction of pockets elude this containment and go on to relax the bulk of the sample (the dark gray and black regions). It is the "frozen" domains of locked spins, awaiting the action of a distant unconstrained pocket, which give rise to the observed long-time relaxation behavior. In contrast, at the higher temperature (Fig. 5), the pockets occur with a higher density, overlapping one another and so greatly reducing the possibility of a pocket becoming trapped. As a result, almost all of the high-temperature sample is relaxed within the short-time domain.

The crossover time t^* is essentially the time it takes the system to "decide" what fraction of relaxing regions are trapped. We have found that the values of t^*, determined as the lower time limit of the applicability of the long-time scaling of $F(t)$, coincide with the distinct minima in a plot of $\gamma(t)=d\{\ln[-\ln(F)]\}/d[\ln(t)]$ vs $\ln(t)$ shown in Fig. 6. (The genesis of this admittedly obscure function $\gamma(t)$ is that *if* $F(t)=\exp[-(t/\tau_L)^{\gamma}]$ then $\gamma(t)$ would be constant and equal to γ.) While we have yet to arrive at a particularly useful interpretation of this observation, it is noteworthy on two counts. First, the striking asymmetry of $\gamma(t)$ about the minimum at t^* presents us with a graphic expression of the difference in relaxation mechanism between the intermediate- and long-time domains. On a more prosaic level, identifying the crossover time as the position of the minimum in $\gamma(t)$ allows us to clear definition of t^*.

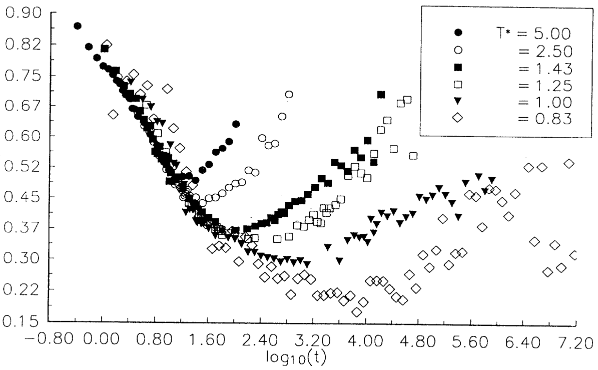

FIG. 6. The function $\gamma(t)=d(\ln\{-\ln[F(t)]\})/d(\ln t)$ vs $\log_{10}(t)$ for a range of T^*. A distinct minimum is observed for each temperature and its position is found to coincide with the crossover time t^*.

This is the physical picture of the process of glassy relaxation in this system, an inhomogeneous process in which (a) pockets, regions in which the configurations satisfy the nonlocal (and nonlinear) kinetic constraints, relax rapidly; (b) the population of the pockets contributing to relaxation is reduced as the process proceeds due to trapping (another consequence of the interplay between fluctuations and kinetic constraints)—this decimation of the number of effective pockets increases markedly with decreasing temperature; and (c) the surviving unconstrained pockets, increasing rare fluctuations in colder samples, relax the remainder of the sample by way of a complex diffusional process. This picture shares much in common with earlier explanations of the β process in terms of localized pockets [10] and of the α process involving the action of diffusing defects [11,12]. In addition to unifying these explanations, this work extends these ideas in two important ways. First, the pockets are defined using the localized *kinetics* rather than the localized *structure,* providing a general criterion of direct relevance to relaxation. Second, this definition, in conjunction with the simplicity of the propagator, provides an explicit process (trapping) by which the density of pockets responsible for long-time relaxation can be obtained.

IV. FROM MECHANISM TO PREDICTIONS

This picture permits a number of quantitative predictions.

(i) The time scale for the short-time relaxation τ_s, by definition, involves no cooperativity (as pockets are defined by the local satisfaction of the kinetic constraints) and so should be the time scale of the elementary event, a single flip, and thus τ_s is expected to be proportional to $\exp(2/T^*)$.

(ii) The amplitude of the short-time decay should be proportional to the density of pockets. This density, in turn, is assumed to be proportional to $f(1)$, the probability of finding a flippable spin. By a simple summing of the probabilities of the various local configurations which permit flipping we find that $f(1)=6c^2(1-c)^2$

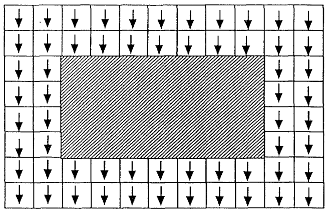

FIG. 7. An example of a "cage" in the fkI model. The enclosing wall of down spins cannot be relaxed as a result of the spin configuration within the shaded region as all the "wall" spins (with the exception of the outer corner spins) have three down neighbors and so cannot flip. The relaxation of such a region must come from outside the cage.

$+4c^3(1-c)+c^4$ (see Ref. [7] for details).

(iii) The fraction of the system which has been relaxed by the short-time process, i.e., $1-F(t^*)$, should be just the fraction of the total area covered by the pockets of rapidly relaxing spins. Consider the following simple argument. The change in $1-F(t^*)$ with $f(1)$ (proportional to the density of pockets) is assumed to be

$$\frac{d[1-F(t^*)]}{df(1)}=bF(t^*)\ , \tag{3}$$

where, on the right-hand side, b corresponds to the average area of a pocket (assumed to be independent of T^*) while the presence of $F(t^*)$ accounts for the fraction of the pocket which overlaps existing pockets. The prediction, then, is that $F(t^*)=\exp[-bf(1)]$.

Finally, (iv), the long-time behavior is dominated by the fraction of the pockets which have avoided being trapped. Trapping results when a region of lattice sites is surrounded by a rectangular wall of down spins two layers thick. (In such a wall, an example of which is shown in Fig. 7, a spin will have three neighbors which are down and so be unable to flip.) The probability p_{cage} that a given spin does not lie inside such confines of any size has been shown [7] to be $p_{\text{cage}}=\exp\{(1-c)^8/\ln[(1-c)^8]\}$. The density C of regions responsible for global relaxation is then the fraction of flippable sites, $f(1)$, which avoid entrapment, i.e., $C=f(1)p_{\text{cage}}$. As C is directly related to the longest length scale in the system (i.e., the average distance between mobile pockets), it seems reasonable to propose that it determines the longest time scale in the system τ_L.

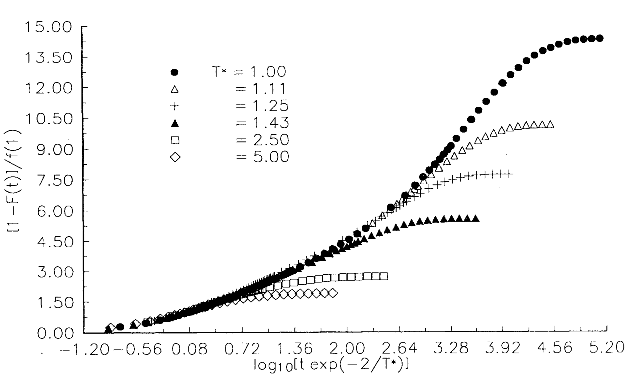

FIG. 8. A plot of the amplitude-scaled relaxation function $[1-F(t)]/f(1)$ [with $f(1)$ being the fraction of flippable sites] vs the scaled time $t\exp(-2/T^*)$. The data from different temperatures fall upon a common curve at short and intermediate times, supporting the predicted scaling described in the text.

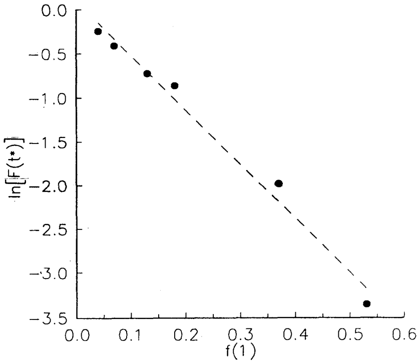

FIG. 9. The plot of the log of the relaxation amplitude $\ln[F(t^*)]$ at the crossover time vs $f(1)$, the density of flippable sites, is well described by a straight line. This is in agreement with the overlap model expressed in Eq. (3). The parameter b in this equation is found to be ≈ 6.

Now we test these predictions. Starting with the long-time or α process [and prediction (iv)], τ_L is found to be very well described over six orders of magnitude by a simple power-law dependence on the density C of mobile pockets, $\tau_L \propto C^{-3.8}$. The connection between this result and that of the defect diffusion model has been discussed elsewhere [7]. To check the predictions for the short-time behavior, $1-F(t)$, the fraction of spins which have flipped by time t is divided by $f(1)$ [using prediction (ii)], and plotted against the log of a reduced time $t\,x\exp(-2/T^*)$ [from prediction (i)] in Fig. 8. The curves at different temperatures are observed to collapse onto a common curve over the short-time domain, demonstrating the validity of the proposed time and amplitude scaling. To test for the predicted exponential dependence of $F(t^*)$ on the pocket density [prediction (iii)], $\ln[F(t^*)]$ is plotted against $f(1)$ in Fig. 9. The data lie close to a straight line, in good agreement with the prediction of Eq. (3).

V. CONCLUSIONS AND DISCUSSION

In conclusion, we have presented an explicit physical picture of the collective mechanism responsible for the characteristic relaxation behavior of a model glass over intermediate and long times. The success of the various predictions provides strong support for this unified picture of the α and β relaxation. A number of specific consequences of the observed mechanism are worth noting. (i) The non-Arrhenius temperature dependence of τ_L arises from the reduction of the number of effective pockets by trapping. If no significant reduction occurs within the temperature window set by the accessible time scales, the relaxation time will exhibit a simple Arrhenius dependence. (ii) The role of the cooperative effects in the short-and long-time regions is distinctly different. In the former it sets the amplitude of the relaxation function, while in the latter it determines the time scale.

While the quantitative analysis of the spatial fluctuations in the relaxation rates is specific to the fkI model, we can still extract a number of predictions which might be of more general application. In terms of the density of "pockets," now generalized to localized regions of rapid structural relaxation, our results suggest that the average relaxation time τ_L scales with the density of the *mobile* pockets as a power law, while, at shorter times, the amplitude of the relaxation function is proportional to the total "pocket" density. Testing these ideas on a real glass requires information about the spatial extent of kinetic fluctuations. It is hoped that these ideas might help focus the experimental challenge posed by this aspect of complex glass dynamics.

The recognition that the fluctuations which govern dynamics take the form of discrete objects, in this case pockets and walls, appears to be a feature common to other kinetic phenomena involving fluctuations in nonlinear fields [13]. Examples include vortices and plumes in descriptions of turbulent fluids [14] and defects in solid-state relaxation [15]. One point which emerges clearly from this study is that the long-time relaxation is governed by fluctuations whose density drops rapidly with decreasing temperature. The special theoretical problems posed by kinetic phenomena dominated by rare events (e.g., nucleation and crack propagation) have typically been handled by including the important fluctuations by hand. In the case of the glass-forming liquid, however, these fluctuations arise from the subtle interplay of dynamic constraints and configurational fluctuations and have yet to be characterized sufficiently for this approach.

We note that the application of relaxation-time maps to the simulations of more realistic models of molecular liquids is straightforward. In going from a model of discrete variables to one with continuous variables, some sort of threshold must be chosen in order to define a local first-passage time. Work is currently underway on the spatial structure of the slow-rotational and translational relaxation in molecular-dynamic simulations of a dense 2D molecular liquid [16].

ACKNOWLEDGMENTS

It is a pleasure to thank Alf Sjölander for some valuable discussions and particularly for urging me to look for a β process and Henk Lekkerkerker for his warm hospitality during my stay at Utrecht and for many stimulating discussions on glasses.

[1] C. A. Angell, J. Non-Cryst. Solids **73**, 1 (1985).
[2] N. J. Tao, G. Li, and H. Z. Cummins, Phys. Rev. B **45**, 686 (1992); W. Krack, F. Mezei, and B. Farago, Europhys. Lett. **7**, 529 (1988); W. van Megen and P. N. Pusey, Phys. Rev. A **43**, 5429 (1991).
[3] G. Wahnström, Phys. Rev. A **44**, 3752 (1991); L. J. Lewis, Phys. Rev. B **44**, 4245 (1991).
[4] W. Götze and L. Sjögren, Rep. Prog. Phys. **55**, 241 (1992).
[5] K. Schmidt-Rohr and H. W. Spiess, Phys. Rev. Lett. **66**, 3020 (1991).
[6] G. H. Fredrickson and S. A. Brawer, J. Chem. Phys. **84**, 3351 (1986).
[7] S. Butler and P. Harrowell, J. Chem. Phys. **95**, 4454 (1991).
[8] K. L. Ngai, Comments Solid State Phys. **9**, 127 (1979).
[9] M. Foley and P. Harrowell, J. Chem. Phys. **98**, 5069 (1993).
[10] G. P. Johari, in *Molecular Dynamics and Relaxation Phenomena in Glasses,* edited by Thomas Dorfmüller and Graham Williams, Lecture Notes in Physics Vol. 277 (Springer-Verlag, Berlin, 1986), p. 90.
[11] S. H. Glarum, J. Chem. Phys. **33**, 1371 (1960).
[12] J. T. Bendler and M. F. Schlesinger, J. Phys. Chem. **96**, 3970 (1992).
[13] Ya. B. Zeldovich, A.A. Ruzmaikin, and D. D. Sokoloff, *The Almighty Chance* (World Scientific, Singapore, 1990).
[14] See references in *Whither Turbulence? Turbulence at the Crossroads,* edited by John L. Lumley, Lecture Notes in Physics Vol. 357 (Springer-Verlag, Berlin, 1990).
[15] N. B. Tufillaro, R. Ramshankar, and J. P. Gollub, Phys. Rev. Lett. **62**, 422 (1989).
[16] S. Priyadarshy and P. Harrowell (unpublished).